A model of intracellular pH control

Soroush Safaei[1], Peter Hunter[1] and Walter Boron[2]

[1]Auckland Bioengineering Institute, University of Auckland, New Zealand
[2]Department of Physiology and Biophysics, Case Western Reserve University, Cleveland, USA

Contributions to paper: SS and PH implemented the models from the original paper, wrote them in bond graph form and then coded them in CellML for solution with OpenCOR. WB ensured that the *Physiome* models are consistent with his original equations. All three authors contributed to the writing of the paper.

Introduction

In 1976 Boron and De Weer published their landmark paper on "Intracellular pH transients in squid giant axons caused by CO_2, NH_3, and metabolic inhibitors" [1]. This paper used an experimental giant squid preparation and a mathematical model of pH buffering and the transport of protons, bicarbonate and CO_2 to establish the experimental evidence for active control of pH by a membrane proton pump. The paper reported on the consequences of exposing the axons first to elevated CO_2, then to elevated NH_3, and finally to the metabolic inhibitors, cyanide, azide and dinitrophenoxide (DNP).

In the first experiment, following exposure of the cells to elevated CO_2, intracellular CO_2 rapidly equilibrates with the extracellular CO_2, and intracellular H^+ and HCO_3^- therefore accumulate from the carbonic anhydrase reaction. Since HCO_3^- rapidly leaves the cell down the newly reversed $[HCO_3^-]$ electrochemical gradient (thereby increasing the drive for CO_2 entry), the accumulating H^+ results in a lowered intracellular *pH* (pH_i). The expectation was that prolonged exposure to CO_2 would cause a continued drop in pH_i, but in fact an *alkaline* drift was observed, leading to the postulate of active pumping of H^+ out of the cell at a rate that exceeds the passive shuttling by the CO_2/HCO_3^- couple. Following removal of external CO_2, intracellular CO_2 diffuses out while intracellular HCO_3^- combines with H^+ to leave the cell as CO_2. In the absence of a H^+ pump, the entire intracellular H^+ load associated with CO_2 entry would be expected to be removed. In fact pH_i was observed to overshoot its resting value by an amount consistent with the net removal of H^+ by the pump.

In the second experiment, following exposure to elevated NH_4^+, the intracellular environment becomes alkaline as NH_3 enters and hydrates to form NH_4^+ and OH^-. Additional passive NH_4^+ entry down its electrochemical gradient therefore opposes the NH_3 entry and slightly reduces the pH_i increase. These effects and the subsequent pH_i undershoot when external NH_4^+ is removed, are also consistent with the proposed model that includes an active proton pump.

Finally, exposure of the cells to (sequentially) cyanide, DNP and azide resulted in intracellular acidosis, consistent with metabolic inhibition of the proton pump.

In this paper we recast the equations from the Boron and De Weer paper using the Physiome modelling standards in order to ensure that the model reproduces the graphs in the original paper and is reusable in modular form for incorporation into other models that require intracellular pH control. The curated and annotated model is made available in a form that users can immediately run with OpenCOR[1] to understand the model and to explore the effect of parameter changes.

[1] www.opencor.ws

The carbonic anhydrase reaction and buffering of H^+ by weak acids and weak bases

The formation of bicarbonate (HCO_3^-) from CO_2 by hydration is catalysed by carbonic anhydrase (CA):

$$CO_2 + H_2O \Leftrightarrow H_2CO_3 \overset{CA}{\Leftrightarrow} HCO_3^- + H^+ \qquad (1)$$

where, at steady state, the relative concentrations obey mass-action and $K_{CO_2} = \frac{[HCO_3^-][H^+]}{[CO_2]}$ is the equilibrium coefficient in units of mM. Note that the formation of carbonic acid (H_2CO_3) is slow (~15s) in the absence of CA but very fast when CA present. Taking logs and using Henry's law, $[CO_2] = s.p_{CO_2}$, where s is the solubility coefficient for CO_2 in the relevant fluid, yields the Henderson-Hasselbalch equation for the CO_2/HCO_3^- buffer system [2]:

$$pH = pK + \log\frac{[HCO_3^-]}{s.p_{CO_2}}, \text{ where } pH = -\log_{10}[H^+] \text{ and } pK = -\log_{10} K$$

The dissociation of cationic weak acid (BH^+) to weak base (B) is governed by the reaction

$$BH^+ \Leftrightarrow B + H^+ \text{ (e.g. } NH_4^+ \Leftrightarrow NH_3 + H^+) \text{ and at equilibrium: } K_B = \frac{[B][H^+]}{[BH^+]}$$

The dissociation of uncharged weak acid (HA) to anionic weak base (A^-) is governed by

$$HA \Leftrightarrow A^- + H^+ \text{ (e.g. } HCO_3^- \Leftrightarrow OH^- + CO_2) \text{ and at equilibrium: } K_A = \frac{[A^-][H^+]}{[HA]}$$

These reactions hold on both sides of a cell membrane, with the same equilibrium constants on both sides. The neutral species (B and HA) move freely down their concentration gradients to equilibrate at equal concentration on either side of the membrane.

The charged species (BH^+, A^- and H^+) move down their concentration gradients (within a membrane protein channel) until equilibrating with their Nernst potentials[2]:

$$E_{BH} = \frac{RT}{F}\ln\frac{[BH^+]_o}{[BH^+]_i}, \quad E_A = \frac{RT}{F}\ln\frac{[A^-]_o}{[A^-]_i}, \quad E_H = \frac{RT}{F}\ln\frac{[H^+]_o}{[H^+]_i}$$

When the reaction $BH^+ \Leftrightarrow B + H^+$ is in equilibrium on both sides of the membrane, and both K_B and $[B]$ are the same on both sides (free permeation of the uncharged molecule),

$$K_B = \frac{[B][H^+]_o}{[BH^+]_o} = \frac{[B][H^+]_i}{[BH^+]_i} \text{ or } \frac{[H^+]_o}{[H^+]_i} = \frac{[BH^+]_o}{[BH^+]_i} \quad \therefore E_{BH} = E_H$$

Similarly, when the reaction $HA \Leftrightarrow A^- + H^+$ is in equilibrium, and $[HA]_0 = [HA]_i = [HA]$,

$$K_A = \frac{[A^-]_o[H^+]_o}{[HA]} = \frac{[A^-]_i[H^+]_i}{[HA]} \text{ or } \frac{[A^-]_o}{[A^-]_i} = \frac{[H^+]_i}{[H^+]_o} \quad \therefore E_A = -E_H$$

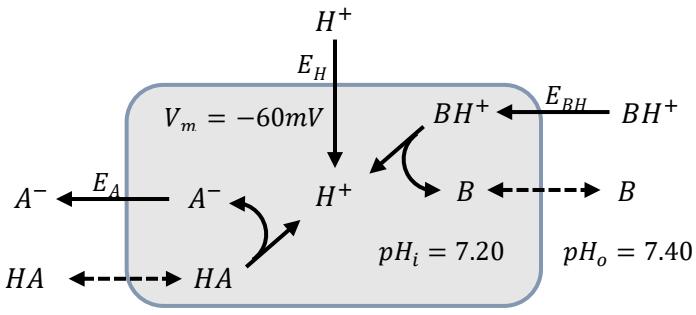

[2] R≈8.4 J.mol^{-1}.K^{-1} and F≈0.96x10^5 C.mol^{-1}, therefore at T=298K (25°C), RT≈2.5kJ.mol^{-1} and RT/F≈25mV.

Modelling reactions and transmembrane fluxes with bond graphs

The bond graph formalism [3] is a useful way to ensure that the formulation of a model conserves both mass and energy and maintains thermodynamic consistency. We define a chemical potential $\boldsymbol{\mu}$ (*J.mol*$^{-1}$) and a molar flow rate $\boldsymbol{v} = \dot{\boldsymbol{q}}$ (*mol.s*$^{-1}$) such that the product $\boldsymbol{\mu}.\boldsymbol{v}$ is power (*J.s*$^{-1}$). For a dilute system, $\boldsymbol{\mu_1} = \mu_1^0 + RT \ln \frac{q_1}{q_{tot}}$ (*J.mol*$^{-1}$), where $\boldsymbol{q_1}$ is the number of moles of substance 1 and q_{tot} is the total number of moles of all substances in the mixture. This can be written $\boldsymbol{\mu_1} = RT \ln K_1 \boldsymbol{q_1}$ (*J.mol*$^{-1}$), where $K_1 = \frac{1}{q_{tot}} e^{\mu_1^0/RT}$ (*mol*$^{-1}$) and RT =2.5 *kJ.mol*$^{-1}$ at 25°C (298K). Note that this is a thermodynamic relationship and K_1 is a thermodynamic parameter. Now consider a reaction

$$\boldsymbol{q_1} \underset{A^r}{\overset{A^f}{\rightleftharpoons}} \boldsymbol{q_2} \qquad \text{or} \qquad \boldsymbol{q_1} \xrightarrow[\boldsymbol{v_1}]{\boldsymbol{\mu_1} = A^f} \text{Re} \xrightarrow[\boldsymbol{v_2}]{\boldsymbol{\mu_2} = A^r} \boldsymbol{q_2}$$

where A^f and A^r are the forward and reverse affinities, represented by the dissipative reaction component Re. The 'reaction rate' or molar flow is given by the Marcelin-de Donder formula: $\boldsymbol{v} = v^+ - v^-$, where $v^+ = \kappa e^{A^f/RT}$ and $v^- = \kappa e^{A^r/RT}$ and hence $\boldsymbol{v} = \kappa \left(e^{A^f/RT} - e^{A^r/RT} \right)$ or $\boldsymbol{v} = \kappa \left(e^{\boldsymbol{\mu_1}/RT} - e^{\boldsymbol{\mu_2}/RT} \right)$.

The solutes and dissolved gases are given the symbol $\boldsymbol{q_i}$ with units of millimoles per litre (10^{-3} mol.L^{-1} or mM) and the flux of solutes undergoing a reaction is denoted by $\boldsymbol{v_1}$ (mM.s^{-1}).

For example, the Bond Graph diagram representing equation (1), with the concentrations of dissolved CO_2, bicarbonate and hydrogen ions given by $\boldsymbol{q_1} = [CO_2] = s.p_{CO_2}$, $\boldsymbol{q_2} = [HCO_3^-]$ and $\boldsymbol{q_3} = [H^+] = 10^{-pH}$, is:

$$\boldsymbol{q_1} \xrightarrow{\boldsymbol{\mu_1}} \text{Re1} \xrightarrow{\boldsymbol{\mu_2}} \boldsymbol{v_1} \begin{cases} \rightarrow \boldsymbol{q_2} \\ \rightarrow \boldsymbol{q_3} \end{cases}$$

where mass conservation requires $\dot{\boldsymbol{q}}_1 = -\boldsymbol{v_1}$, $\dot{\boldsymbol{q}}_2 = \boldsymbol{v_1}$ and $\dot{\boldsymbol{q}}_3 = \boldsymbol{v_1}$. The reaction Re1 is defined by the relation

$$\boldsymbol{v_1} = -\kappa_1 + \kappa_1 K_2 K_3 \boldsymbol{q_2} \boldsymbol{q_3}$$

where $\boldsymbol{\mu_1} = -K_1 \boldsymbol{q_1}$ and $\boldsymbol{\mu_2} = K_1 \boldsymbol{q_1}$. Note that κ has units of *mol.s*$^{-1}$ and that this is an empirical resistive (dissipative) constitutive relation. The direction of flow is determined by the solution to ensure that the second law of thermodynamics is satisfied ($\Delta G = \Delta H - T\Delta S < 0$).

For transmembrane fluxes, we let $\boldsymbol{q}$ have units *mol.m*$^{-3}$ (molar concentration) and $\boldsymbol{v}$ have units *mol.m*$^{-2}$*.s*$^{-1}$ (flux per unit membrane area). The surface area to volume ratio ρ (*m*$^{-1}$) is used to link membrane fluxes with intracellular volume fluxes)

The flux from passive diffusion is $\boldsymbol{v} = \kappa(\boldsymbol{q_1} - \boldsymbol{q_2})$, where κ (*m.s*$^{-1}$) is the permeability coefficient.

Applying this constitutive relation to the two uncharged species HA and B gives

$$\boldsymbol{v_1^{HA}} = \kappa_{v1} \left(\boldsymbol{q_1^{HA_o}} - \boldsymbol{q_2^{HA_i}} \right) \qquad \text{and} \qquad \boldsymbol{v_6^{B}} = \kappa_{v6} \left(\boldsymbol{q_7^{B_i}} - \boldsymbol{q_8^{B_o}} \right)$$

Membrane voltage $\boldsymbol{\mu_E}$ and RT/zF both have units *J/C* (or *Volts*). We define a quantity $\boldsymbol{\varepsilon} = zF\boldsymbol{\mu_E}/RT$ as a dimensionless membrane potential. Solution of the 1D Nernst-Planck equation for an ion channel pore gives the molar flow of ions passing through the channel as

$$\boldsymbol{v} = \kappa_\varepsilon \boldsymbol{\varepsilon}. \frac{\boldsymbol{q_1} - \boldsymbol{q_2}.e^{-\boldsymbol{\varepsilon}}}{1 - e^{-\boldsymbol{\varepsilon}}}, \qquad \text{where } \kappa_\varepsilon \text{ (}m.s^{-1}\text{) is the channel permeability.}$$

Applying this Goldman-Hodgkin-Katz (GHK) constitutive relation to the 3 charged species H^+, $BH^+$and A^- gives

$$v_3^{A^-} = \kappa_{v3}.\varepsilon.\frac{q_3^{A_i^-} - q_4^{A_o^-}.e^{-\varepsilon}}{1-e^{-\varepsilon}}, \quad v_4^{BH^+} = \kappa_{v4}.\varepsilon.\frac{q_5^{BH_o^+} - q_6^{BH_i^+}.e^{-\varepsilon}}{1-e^{-\varepsilon}}, \quad v_7^{H^+} = \kappa_{v7}.\varepsilon.\frac{q_9^{H_i^+} - q_{10}^{H_o^+}.e^{-\varepsilon}}{1-e^{-\varepsilon}}$$

The weak acid and base reactions within the cell are:

$$HA \Leftrightarrow A^- + H^+ \text{ and } BH^+ \Leftrightarrow B + H^+$$

where $v_2^{HA_i} = \kappa_{v2}\left(K_2 q_2^{HA_i} - K_3 K_9 q_3^{A_i^-} q_9^{H_i^+}\right)$

and $v_5^{BH_i^+} = \kappa_{v5}\left(K_6 q_6^{BH_i^+} - K_7 K_9 q_7^{B_i} q_9^{H_i^+}\right)$

Note that κ_{v2} & κ_{v5}, and v_2 & v_5, all have units *mol.m*$^{-3}$*.s*$^{-1}$.

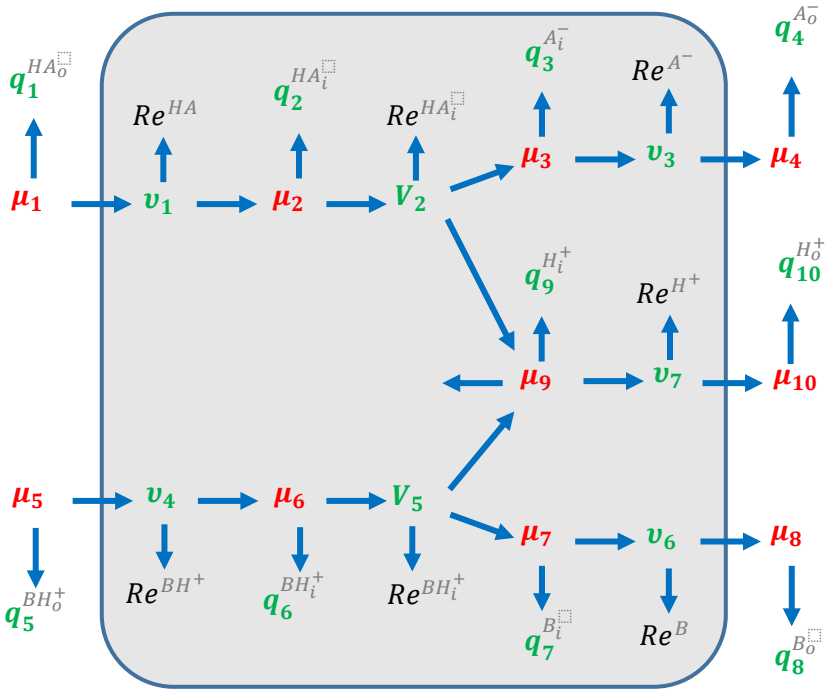

The conservation relations are:

$$\dot{q}_1^{HA_o} = -v_1^{HA}$$
$$\dot{q}_2^{HA_i} = v_1^{HA} - v_2^{HA}$$
$$\dot{q}_3^{A_i^-} = v_2^{HA} - v_3^{A^-}$$
$$\dot{q}_4^{A_o^-} = v_3^{A^-}$$
$$\dot{q}_5^{BH_o^+} = -v_4^{BH^+}$$
$$\dot{q}_6^{BH_i^+} = v_4^{BH^+} - v_5^{BH^+}$$
$$\dot{q}_7^{B_i} = v_5^{BH^+} - v_6^{B}$$
$$\dot{q}_8^{B_o} = v_6^{B}$$
$$\dot{q}_9^{H_i^+} = v_2^{HA} + v_5^{BH^+} - v_7^{H^+}$$
$$\dot{q}_{10}^{H_o^+} = v_7^{H^+}$$

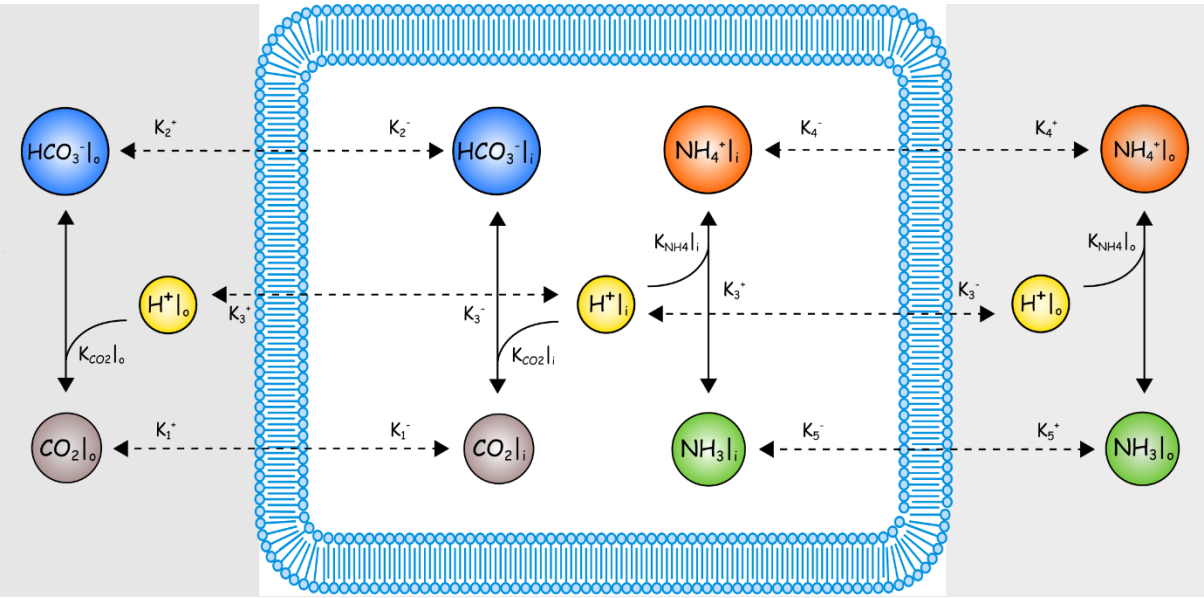

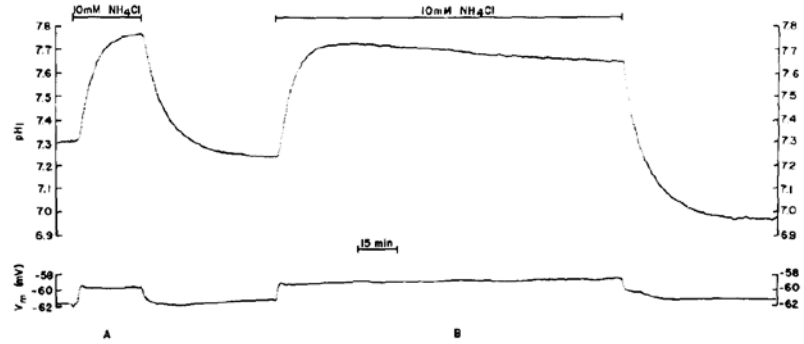

Figure 3. (A) Effect of short-term NH_4Cl exposure on pHi and membrane potential. (B) Effect of long-term NH_4Cl exposure on pH_i and membrane potential.

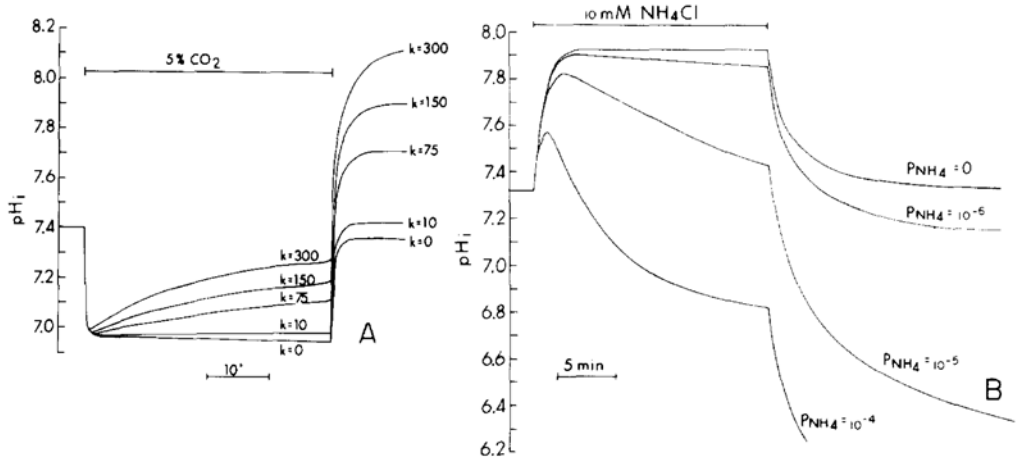

(A) Computer-simulated pH~ time-course during and after exposure to CO_2. Variations in k, the proton pump rate constant (given in s^{-1}), result in changes in the plateau phase slope and the amount of overshoot. When k = 0 (no pumping) pH~ actually declines in the plateau phase and fails short of the initial pH~ upon removal of the CO~. In these plots, pKa' = 6.00, fl = -26 mM, pHCO3 • 5.10^{-7} tin/s, Pco~ = 6.10^{-3} cm/s, pH_o = 7.70, P_{CO2} = 37 mm Hg (5% CO_2), T = 23°, and fiber diameter = 500/zm. (B) Computer-simulated pH~ time-course during and after exposure to NH4CI. Variations of PNm, the permeability of the membrane to NH_4^+ (given in $cm.s^{-1}$), produce changes in the plateau phase slope and the amount of undershoot. When PNm = 0, the plateau phase is nearly horizontal, and pH, returns to exactly the initial pH~ after removal of external NH4C1. When PNm

is very large proton shuttling takes place at a very rapid pace and pH, soon approaches the value predicted from Donnan theory. In these plots, pKa' = 9.50,/3 = -9mM, PNH3 = 6.10^{-3} cm/s, $[NH_4Cl]_o$ = 10mM, pH,, = 7.70, k (H^+ pump rate constant) = 0, T = 23°, and fiber diameter = 500 ~m.

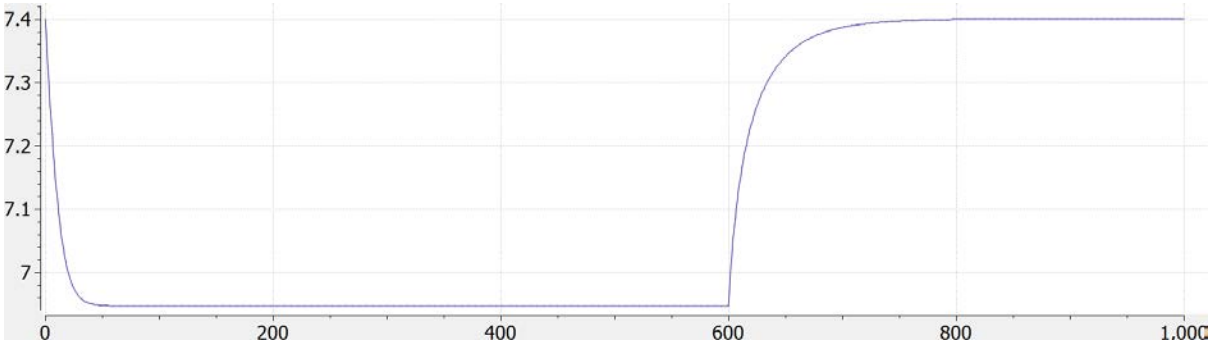

References

1. Boron WF and De Weer P. Intracellular pH transients in squid giant axons caused by CO_2, NH_3, and metabolic inhibitors. *Journal of General Physiology*, Vol. 67, pp 91-112, 1976.
2. Boron WF and Boulpaep E. Medical Physiology. 3rd Edition, Elsevier, 2016.
3. de Bono B, Safaei S, Grenon P and Hunter, P. Meeting the multiscale challenge: representing physiology processes over ApiNATOMY circuits using bond graphs. Interface Focus 2017.